LEP data and the stability of the potential confront the mSUGRA model

Amitava Datta [a], Abhijit Samanta [b,c]

[a] *Department of Physics, Jadavpur University, Kolkata 700 032, India*
[b] *Saha Institute of Nuclear Physics, 1/AF Bidhan Nagar, Kolkata 700 064, India*
[c] *Department of Physics, University of Calcutta, Kolkata 700 009, India*

Abstract

The requirement that the supersymmetric scalar potential be stable in the minimal supergravity (mSUGRA) model imposes an upper bound on the universal gaugino mass $m_{1/2}$ as function of the common scalar mass m_0. Combining this with the experimental lower bound on $m_{1/2}$ from LEP data, we find a new lower bound on m_0, stronger than the one that comes from experimental data alone. If the corresponding upper limits on the superparticle masses, derived in this Letter, are found to be violated at Tevatron Run II or at the LHC, it would imply that we are living on a false vacuum. Special attention has been paid in estimating the uncertainties in these predictions due to the choice of the renormalization scale. The implications of our limits for the constraints obtained by indirect methods (SUSY dark matter, $g-2$ of the muon, $b \to s\gamma \ldots$) are briefly discussed.
© 2004 Elsevier B.V. Open access under CC BY license.

PACS: 12.60.Jv; 14.80.Ly; 14.80.Cp

Currently supersymmetric theories are among the best motivated extensions of the Standard Model (SM) [1]. The most general one at low energy is the Minimal Supersymmetric extension of the Standard Model (MSSM). However, its phenomenological study is almost impossible due to large number of free parameters. Almost all of them arise due to our failure to discover the precise mechanism of supersymmetry (SUSY) breaking. Currently there are several popular models of supersymmetry breaking. The theoretical assumptions in these models reduce the parameter space. The most well-studied model is the minimal supergravity (mSUGRA) model [2] with radiative electroweak symmetry breaking [3]. This model has only five free parameters. They are the common scalar mass (m_0), the common gaugino mass ($m_{1/2}$), the common

E-mail addresses: adatta@juphys.ernet.in (A. Datta),
abhijit@anp.saha.ernet.in (A. Samanta).

trilinear coupling (A_0), the ratio of vacuum expectation values of two Higgs field ($\tan \beta$) and the sign of μ, the higgsino mass parameter.

The mSUGRA model has been confronted with the data from LEP as well as from Run I of the Tevatron collider. Such efforts have resulted in some useful lower bounds on these parameters most notably on m_0 and $m_{1/2}$ [4–7]. In this Letter we shall be concerned mainly with the limits obtained by the ALEPH Collaboration on the mSUGRA parameter space [4]. The results obtained by the other LEP groups are similar but some of them do not strictly follow the mSUGRA scenario.

Unfortunately mSUGRA does not predict quantitative upper bounds on these parameters, which could make this model falsifiable in the near future. Of course there are upper bounds based on naturalness arguments [8]. These bounds, however, crucially depends on the value of the fine tuning parameter which, though intuitively appealing, is rather difficult to quantify.

It is, therefore, rather tempting to reexamine the constraints obtained from the stability of the supersymmetric scalar potential [9–11]. It has been demonstrated in the past that these constraints leads to upper bounds on $m_{1/2}$ as a function of m_0 [10,11]. Useful constraints also emerge within the framework of anomaly mediated supersymmetry breaking and other models [12].

Admittedly these bounds can be evaded by assuming that we live in a false vacuum with a life time larger than the age of the universe [13]. Yet such bounds are important. If they are found to be violated after the discovery of SUSY be it at Tevatron Run II or at the LHC, it must be accepted within the mSGRA scenario that the universe is indeed built on a false vacuum.

The unbounded from below (UFB) [10] constraint imposes an upper limit on $m_{1/2}$ (denoted by $m_{1/2}^{\max}$) as function of m_0 (to be explained below). Combining this with the experimental lower bound denoted by $m_{1/2}^{\min}$ from LEP data [4], we find a strong lower bound on m_0 (denoted by $m_0^{\min}$) stronger than the one that comes from experimental data alone. This can be translated into a stronger lower bound on slepton mass. Using the lower bound (from experimental data) and upper bound (from the UFB bound) on $m_{1/2}$ for a given m_0 we derive upper and lower bounds on var-

ious super particle masses for fixed slepton masses. This prediction can be tested in the next round of experiments.

To make this Letter self contained, we briefly discuss the most important, model independent unbounded from below-3 (UFB3) constraint obtained by considering a certain direction in the field space [10]. The scalar potential in this direction is given by

$$
\begin{aligned}
V_{\text{UFB3}} = {} & \big[m_{H_u}^2 + m_{L_i}^2 \big] |H_u|^2 \\
& + \frac{|\mu|}{\lambda_{E_j}} \big[m_{L_j}^2 + m_{E_j}^2 + m_{L_i}^2 \big] |H_u| \\
& - \frac{2 m_{L_i}^4}{g'^2 + g^2},
\end{aligned}
\tag{1}
$$

where g' and g are normalized gauge couplings of $U(1)$ and $SU(2)$, respectively, H_u and H_d are the neutral components of the two Higgs doublets, L_i and E_j are the scalar partners of the leptons belonging to the $SU(2)_L$ doublet and singlet, respectively, λ_{E_j} is a Yukawa coupling and i, j are generation indices. Here $i \neq j$.

Note that we could substitute squarks for sleptons in Eq. (1), in which case $i = j$ is allowed. The constraints on the parameter space arise from the requirement

$$
V_{\text{UFB3}}(Q = \hat{Q}) > V_0^{\min}(Q = M_S),
\tag{2}
$$

where $V_0^{\min}$ is the electroweak symmetry breaking minimum of the scalar potential evaluated at the SUSY breaking scale $Q = M_S$ and the scale $\hat{Q}$ is chosen to be $\hat{Q} \sim \text{Max}(g_2|E_j|, g_2|H_u|, \lambda_{\text{top}}|H_u|, g_2|L_i|, M_S) \sim M(\phi)^{\max}$, where $M(\phi)^{\max}$ is the largest eigenvalue of the field dependent mass matrices. The VEVs $|E_j|$ and $|L_i|$ are determined by H_u and some model parameters. The relevant equations can be found in [10]. The UFB3 potential in Eq. (1) is derived from the tree level scalar potential. It is well known that loop corrections to the potential may have important effects (e.g., the predictions from the one loop corrected potential has a reasonably mild scale dependence) [14]. The above choice of $\hat{Q}$ is designed to minimize the magnitude of the loop corrections to the potential which are of the form $\sim M^4(\phi) \ln \frac{M(\phi)^2}{\hat{Q}^2}$. At this scale, therefore, the tree level potential by itself gives fairly reliable results [10,14]. The price that one has to pay for this simplification is a slight complication in the choice of the

scale. While studying V_{UFB3} as a function of H_u, one must select the scale at each step since it is correlated with H_u.

It should be emphasized that the above prescription only gives an order of magnitude estimate of the scale $\hat{Q}$ for a given H_u. In order to carry out practical computations leading to constraints on the parameter space, $\hat{Q}$ is set exactly equal to the maximum of the quantities given in the parenthesis. In the rest of the paper this scale will be referred to as the approximate scale $\hat{Q}_A(H_u)$. This approximation introduces an element of uncertainty in the derived constraints, which will be discussed in detail before the numerical results are presented.

As can be seen from Eq. (1), the regions of the parameter space, where $m^2_{H_u}$ becomes large negative at the required scale $\hat{Q}_A(H_u)$, tends to violate the UFB3 condition (inequality (2)). This is because the first term of Eq. (1) which dominates for moderate and large values of $|H_u|$, could be negative in this case. However, the second term in (1), which is positive definite, may become competitive in certain cases (e.g., for $j = 1$, when the Yukawa coupling in the denominator is small), and a dangerous minimum may be avoided.

The UFB3 potential with sleptons (Eq. (1)) was found to yield the strongest constraint among all the UFB and charge colour breaking (CCB) conditions in the low $\tan\beta$ case [10]. The results were generalized for large $\tan\beta$ scenarios in [11]. In order to get the optimum result, one has to take the largest λ_{E_j} in the second term of Eq. (1), which leads to the choice $E_j = \tilde{\tau}_R$. Now the restriction $i \neq j$ requires $L_i = \tilde{e}_L$ or $\tilde{\mu}_L$ and excludes the choice $\tilde{\tau}_L$. In the low $\tan\beta$ case this restriction, however, is of little consequence since all the left sleptons are degenerate to a very good approximation.

To find the points in the mSUGRA parameter space which violate the UFB3 constraint (inequality (2)), we vary H_u from the grand unification scale (M_G) to M_Z. For each H_u and a chosen set of the five input parameters the approximate scale $\hat{Q}_A(H_u)$, described after inequality (2), is found by an iterative method (see [11] for the details of the procedure). Next we evaluate the function in Eq. (1). At large H_u (i.e., also at large $\hat{Q}_A(H_u)$), the change of $m^2_{H_u}$ from its boundary value m^2_0 at M_G is negligible. Consequently the first term

of Eq. (1), which dominates, is positive and the inequality is satisfied. As H_u is decreased $m^2_{H_u}$ becomes negative. Further lowering of H_u may eventually make the first term sufficiently negative, leading to the violation of inequality (2) for the chosen set of parameters. This set is then excluded. For some sets of parameters V_{UFB3} is found to be violated for a very narrow range of $\hat{Q}_A(H_u)$ values. Since $\hat{Q}_A(H_u)$ is chosen on the basis of an order of magnitude estimate one may wonder whether this choice is the true value of the scale at which conclusions based on the tree level potential are reliable. For some other sets of parameters, however, V_{UFB3} remains approximately flat for a range of values of H_u (or $\hat{Q}_A(H_u)$) and inequality (2) is violated for the entire range. The corresponding parameter set can be ruled out with more confidence. For H_u beyond this range V_{UFB3} rises above $V^{\min}_0$. It may be inferred that for this range of $\hat{Q}_A(H_u)$ values higher order effects are indeed small, the tree level UFB3 potential by itself is fairly scale independent and conclusions based on it are reliable.

The variation of V_{UFB3} with $\log_{10}(\hat{Q}_A(H_u)/\mathrm{GeV})$ is illustrated in Fig. 1, for $m_0 = 140$ GeV, $m_{1/2} = 220$ GeV, $A_0 = 0$, $\tan\beta = 15$ and $\mu > 0$ by the solid curve. The points denoted by the solid triangle and the open circle represent $V^{\min}_0$ in Eq. (2) for $m_{1/2} = 220$ and 250 GeV, respectively. For numerical convenience we have plotted the logarithms of the potential (see the caption of Fig. 1). The behaviour discussed in the last paragraph is clearly demonstrated. It is to be noted that for this set of parameters the UFB3 condition is violated for a very specific value of $\hat{Q}_A(H_u)$, which may not be identical to the true scale where the UFB3 condition should be tested. The set of parameters under consideration, therefore, cannot be excluded with certainty.

Now we are in a position to illustrate the sensitivity of the excluded the parameter space to the choice of the scale. The dashed curve in Fig. 1 is obtained for $m_{1/2} = 250$ GeV, the other parameters being the same as those for the dotted curve. Now the UFB3 condition is violated for a fairly large range of $\hat{Q}_A(H_u)$. The corresponding parameter space can be eliminated with a higher level of confidence.

In view of the above discussions, we have introduced the following prescription to estimate the uncertainties in the limits derived in this Letter due to
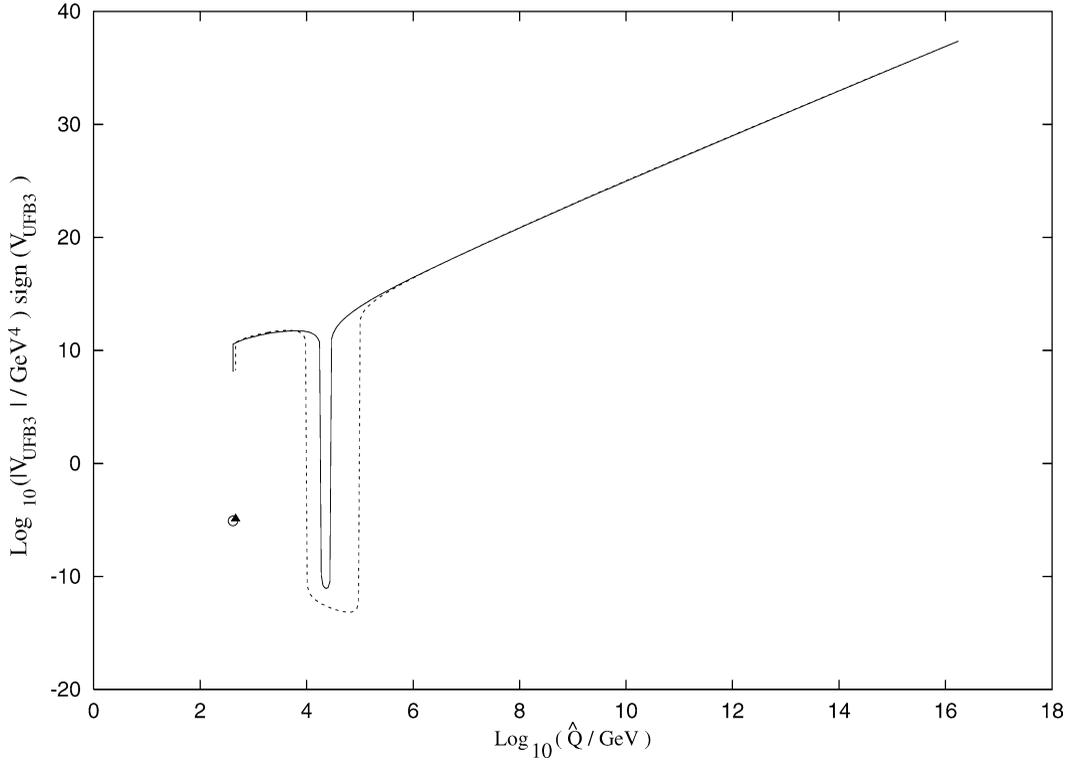
Fig. 1. The variation of $\mathrm{Log}_{10}(|V_{\mathrm{UFB3}}|) \times \mathrm{sign}(V_{\mathrm{UFB3}})$ with the logarithm of the scale $\hat{Q}_A(H_u)$ for $m_{1/2} = 220$ GeV (solid line) and 250 GeV (dotted line). The points denoted by the solid triangle and the open circle indicate the value of $\mathrm{Log}_{10}(|V_0^{\mathrm{min}}|) \times \mathrm{sign}(V_0^{\mathrm{min}})$ for $m_{1/2} = 220$ and 250 GeV, respectively. We set $m_0 = 140$ GeV, $A_0 = 0$, $\tan\beta = 15$ and $\mu > 0$.

the choice of $\hat{Q}_A(H_u)$. In the process of obtaining the upper bound on $m_{1/2}$ for a given m_0, $m_{1/2}$ is increased starting from the LEP lower limit [4]. At a certain $m_{1/2}$ $(= m_{1/2}^{\mathrm{max}})$ the UFB3 condition is violated for the first time at a scale $\hat{Q}_A(H_u)$. Usually this first violation occurs for a very narrow range of $\hat{Q}_A(H_u)$ values. We shall refer to this limit as the optimistic limit (OL). Any $m_{1/2}$ above this value violates the UFB3 condition for a larger range of $\hat{Q}_A(H_u)$ values. This is so because for a given set of $m_0, A_0, \tan\beta$ and sign of μ, a larger $m_{1/2}$ drives $m_{H_u}^2$ in Eq. (1) to larger negative values [11]. Thus, e.g., the UFB3 constraint for a larger $m_{1/2}$ will also be violated at a relatively higher $\hat{Q}_A(H_u)$. The conservative limit (CL) refers to that $m_{1/2}$ for which the UFB3 condition is violated for a range of $\hat{Q}_A(H_u)$ values, $\hat{Q}_A(H_u)^{\mathrm{min}}(= \hat{Q}_A(H_u)^{\mathrm{max}}/10) < \hat{Q}_A(H_u) \leqslant \hat{Q}_A(H_u)^{\mathrm{max}}$. This choice of the range is guided by the conventional understanding of the order of magnitude.

In Fig. 2 we present the allowed region of the m_0–$m_{1/2}$ plane for $\tan\beta = 15$, $A_0 = 0$ and $\mu > 0$. In this figure as well as in the following ones, we have chosen the mSUGRA parameters as in Ref. [4], so that we can combine our theoretical constraints with the experimental limits without any ambiguity. Region I is excluded by the LEP lower limit on the light Higgs mass (m_h), which leads to the strongest experimental constraint in the m_0–$m_{1/2}$ plane in the mSUGRA model. We have used the model independent limits on m_h as a function of the mixing parameters obtained by the ALEPH Collaboration (see Fig. 4 of Ref. [15]) to reconstruct the upper edge of region I, which represents the lower limits on $m_{1/2}$ for different m_0 values. Region IV is excluded by the requirement that the lightest neutralino be the LSP which leads to an upper bound on $m_{1/2}$ for a given m_0. Thus region II and III represent the allowed parameter space (APS) after imposing the experimental and the neutralino LSP constraints.
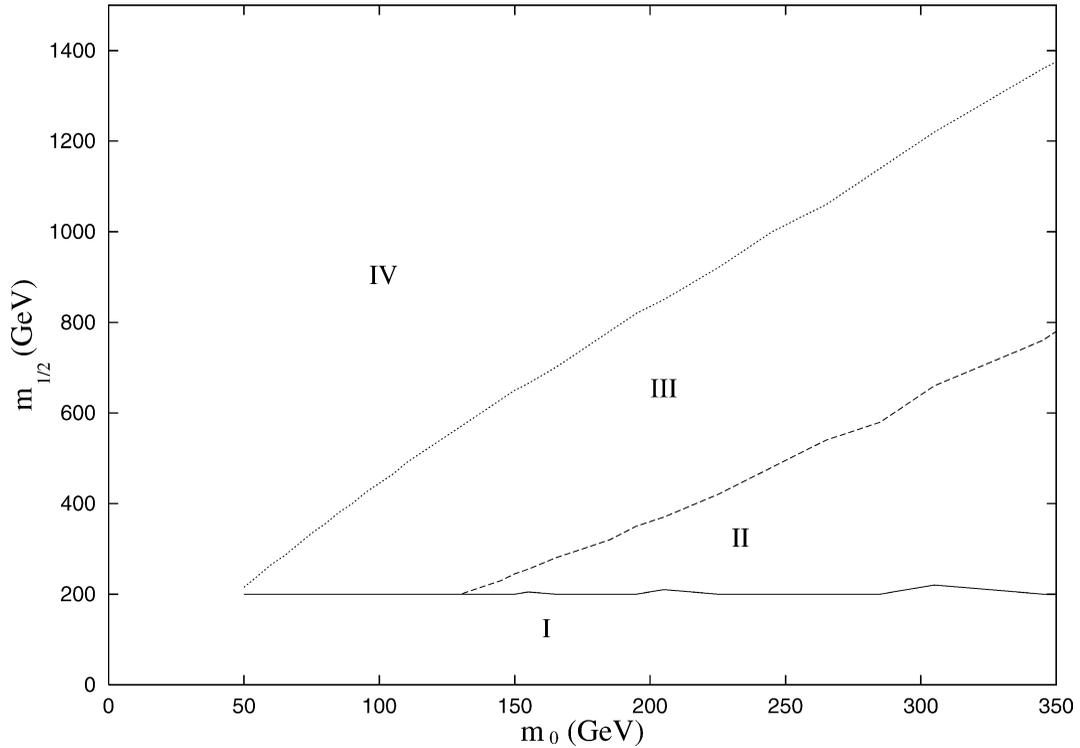
Fig. 2. The allowed parameter space for $A_0 = 0$, $\tan\beta = 15$ and $\mu > 0$. The region II is allowed. The region III is ruled out from UFB3 constraint. The region I and IV are ruled out from experiment and neutralino LSP condition.

The APS in Fig. 2 is in good agreement with the results of ALEPH Collaboration [4], as can be seen by comparing region I of Fig. 2 with the corresponding region of [4] obtained for the same set of mSUGRA parameters. We have used ISAJET version 7.64 [16] for computing the renormalization group evolution of the mSUGRA parameters and the resulting sparticle spectrum. Since m_h is the most important parameter in constraining the m_0–$m_{1/2}$ parameter space, we have also used the FeynHiggs program [17] to compute the Higgs masses. In the following we shall show that the resulting discrepancy is not very serious by comparing the computed m_h values from the two programs.

We now impose the UFB3 constraint (inequality (2)) and obtain the optimistic upper limit (OL, defined above) on $m_{1/2}$ (denoted by $m_{1/2}^{\max}$) for each m_0. This defines the lower boundary of region III, leaving region II as the only APS. It should be emphasized that the combination of the UFB3 and LEP constraints strengthens the lower bound on m_0 ($m_0^{\min}$) as well.

In the absence of the former constraint this bound is $m_0 \gtrsim 50$ GeV (the point of intersection of the upper edge of region I and the lower edge of region IV), which is strengthened to $m_0 \gtrsim 140$ GeV (the point of intersection of the upper edges of region I and II) when the constraints are combined. The two sets of constraints, therefore complement each other very well. As the future experimental lower bound on $m_{1/2}$ get stronger either from an improved bound on m_h or from the direct searches for gluinos, charginos and neutralinos, $m_0^{\min}$ will also become stronger. As we shall see below this corresponds to indirect lower limits on the masses of the scalar superpartners belonging to the first two generations along with some useful information about the other superparticle masses.

The APS for other choices of $\tan\beta$ and sign of μ are presented in Figs. 3 and 4. In each case we see that the effectiveness of the theoretical and experimental constraints acting in tandem is much better than any one of them operating singly. The lower limit on m_0
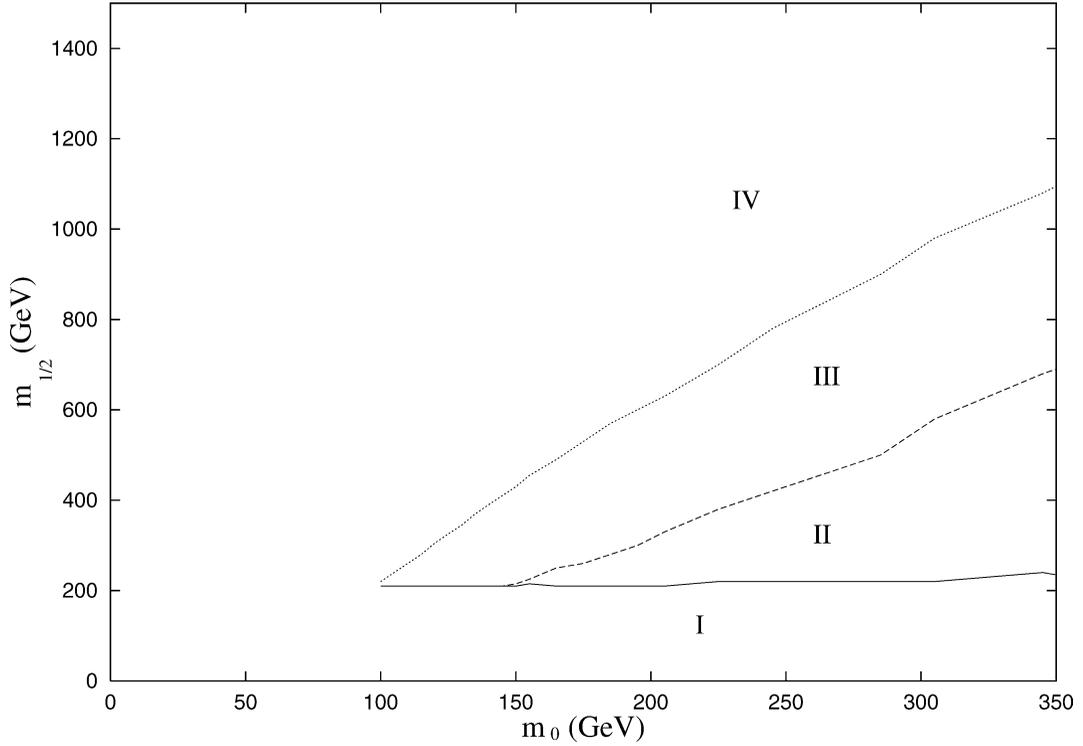
Fig. 3. The same as Fig. 2 with $A_0 = 0$, $\tan\beta = 30$ and $\mu < 0$.

($m_0^{\min}$) in each case is significantly stronger than that obtained from the data alone.

We present in Fig. 5, which is a blown up version of the APS in Fig. 2, the uncertainty in $m_{1/2}^{\max}$ due to the choice of scale for $\tan\beta = 15$, $A_0 = 0$, $\mu > 0$. The thick lines represent information already present in Fig. 2. The optimistic limits (OLs) as defined above are represented by the thick dash-dotted line. The conservative limits (CLs) are given by the line 'a'. Due to the upward shift of the limits $m_0^{\min}$s also get relaxed. It is to be noted that the differences between the OLs and the CLs become more prominent at larger value of m_0.

In Table 1 $m_0^{\min}$ and the corresponding $m_{1/2}$ (i.e., the coordinates of the point of intersection of the upper edges of region I and II which usually determines the lower bound on the slepton mass due to the UFB3 condition in the mSUGRA scenario) are presented for $A_0 = 0$ and several choices of μ and $\tan\beta$. The $m_0^{\min}$ and $m_{1/2}$ presented in the first two columns are obtained from the light Higgs mass (m_h) bound and the neutralino LSP condition. The values in the next two columns represent the optimistic constraints when the

UFB3 condition is added. The last two columns show the conservative limits.

Table 2 reflects the uncertainty in the constraints due to different methods of computing m_h. Here m_h is computed using the two loop corrected formulae in the FeynHiggs program [17], which are presumably more realistic. The new calculation of the Higgs mass shifts the upper edge of region I modestly upwards. As a result the relaxation in $m_0^{\min}$ due to the scale uncertainty is compensated to some extent. The resulting changes in $m_0^{\min}$ and $m_{1/2}$ can be seen by comparing with the corresponding columns in Table 1. We see that the changes are $\lesssim 10\%$ in all cases.

Using the numbers in Table 2, we predict in Table 3 the lower limits on the slepton masses belonging to the first two generations. For low values of $\tan\beta$, even the weaker conservative bounds derived using the UFB3 condition are significantly larger the corresponding results derived from m_h and neutralino LSP constraints only. Detection of sleptons with masses below the above ranges in future experiments would directly signal the existence of minima deeper than the
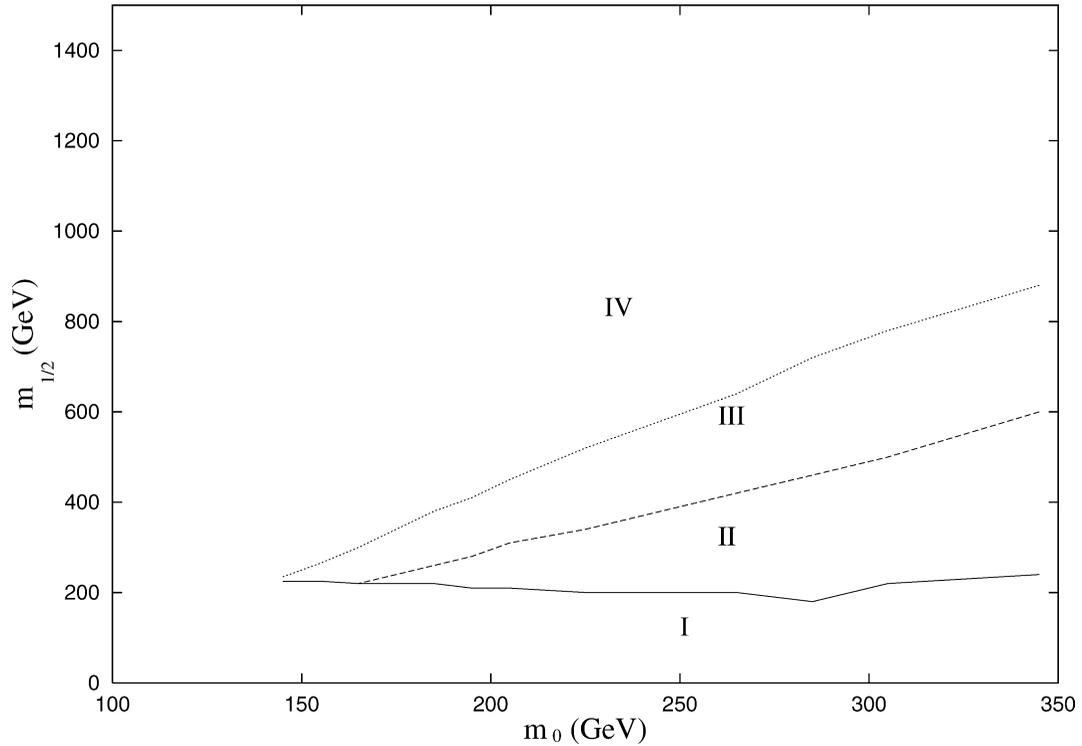
Fig. 4. The same as Fig. 2 with $A_0 = 0$, $\tan\beta = 44$ and $\mu < 0$.

Table 1
The lowest m_0 and the corresponding $m_{1/2}$ using the spectrum generated by the ISASUSY program (see text for further details)

Choice of parameters	$m_{0\,\text{min}}$ (GeV)	$m_{1/2}$ (GeV)	$m_{0\,\text{min}}^{\text{UFB}}$ (GeV)	$m_{1/2}$ (GeV)	$m_{0\,\text{min}}^{\text{UFB}}$ (GeV)	$m_{1/2}$ (GeV)
$\tan\beta = 15$, $\text{sign}(\mu) > 0$	45	200	130	198	115	198
$\tan\beta = 30$, $\text{sign}(\mu) < 0$	98	208	148	208	132	208
$\tan\beta = 44$, $\text{sign}(\mu) < 0$	142	223	166	218	150	224

Table 2
The lowest m_0 and corresponding $m_{1/2}$, when m_h is computed by the FeynHiggs program

Choice of parameters	$m_{0\,\text{min}}$ (GeV)	$m_{1/2}$ (GeV)	$m_{0\,\text{min}}^{\text{UFB}}$ (GeV)	$m_{1/2}$ (GeV)	$m_{0\,\text{min}}^{\text{UFB}}$ (GeV)	$m_{1/2}$ (GeV)
$\tan\beta = 15$, $\text{sign}(\mu) > 0$	51	218	140	218	124	218
$\tan\beta = 30$, $\text{sign}(\mu) < 0$	102	228	159	227	140	227
$\tan\beta = 44$, $\text{sign}(\mu) < 0$	142	223	170	218	148	222

EW symmetry breaking vacuum. The chargino masses corresponding the conservative estimate of the lowest slepton mass are also presented in Table 3. Thus even if sleptons with masses in the ranges shown in Table 3 are found in future experiments, but the lighter chargino mass turns out to be appreciably larger, it would also indicate a violation of the UFB3 bound.

Similar lower limits can also be obtained for the squarks belonging to the first two generations. In mSUGRA the squark mass squared is given by (apart from the relatively unimportant D-term contributions) $m_0^2 + cm_{1/2}^2$, where the dimensionless coefficient c lies between 6.0 and 6.5 [18] for different types of squarks. It is clear that the main contributions to such limits for
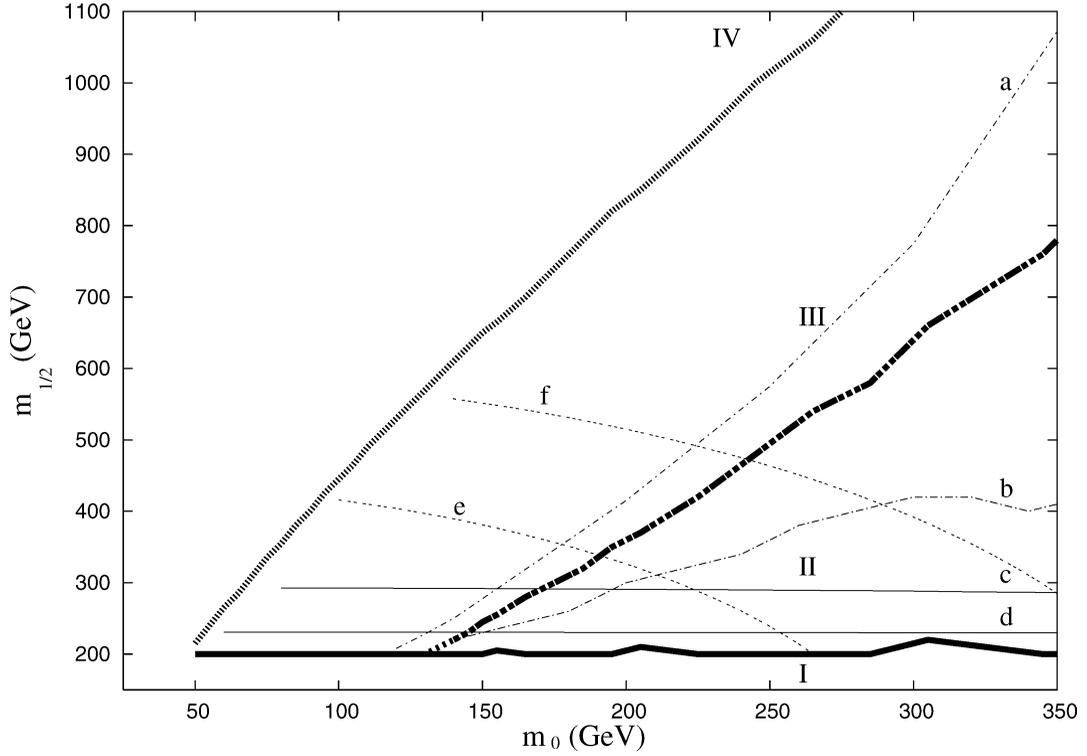
Fig. 5. The blown up version of the allowed parameter space in Fig. 2. The curve labelled by 'a' represents the UFB3 bound after including the scale uncertainty, in the region under the curve 'b' the lighter chargino is the NLSP. The curves 'c' and 'd' are the contours for $m_{\tilde{g}} = 700$ GeV and $m_{\tilde{\chi}^{\pm}} = 160$ GeV; the curves 'e' and 'f' are fixed slepton mass contours for 300 and 400 GeV, respectively.

Table 3
The lower limits on slepton masses belonging to the first two families and the corresponding chargino masses computed using Table 2. The ranges in the mass limits arise due to the scale uncertainty

Combination of parameters	$m_{\tilde{l}L}^{\min}$ (GeV)		$m_{\tilde{l}R}^{\min}$ (GeV)		$m_{\tilde{\chi}^{\pm}}$ (GeV)
	Experiment	UFB	Experiment	UFB	
$\tan\beta = 15$, sign$(\mu) > 0$	163	198–208	105	154–167	156
$\tan\beta = 30$, sign$(\mu) < 0$	190	212–225	139	168–184	161
$\tan\beta = 44$, sign$(\mu) < 0$	212	216–229	169	174–192	157

relatively low m_0 values come from the experimental lower limits on $m_{1/2}$. The stronger $m_0^{\min}$ as determined from the UFB3 condition, will in principle predict a lower bound stronger than the experimental bound. But it may be difficult to distinguish between the two. The shift in mass limits due to the UFB condition, however, may play an important role once precision measurements of these masses are available.

We next discuss the predictions of the UFB3 constraint for slepton masses higher than the lowest allowed values presented in Table 3. For a fixed slepton

mass both upper and lower bounds on several sparticle masses can be computed from the allowed ranges of $m_{1/2}$ presented in Figs. 2–4. As an illustration we present in Fig. 5 the contour of left slepton mass of 300 and 400 GeV. From the points of intersection of contours 'e' and 'f' with the lines representing the UFB3 bound and the experimental bound on $m_{1/2}$, we predict in Table 4 the conservative and optimistic upper bounds and lower bounds on several sparticle masses. It is gratifying to note that the uncertainties in the upper limits due to the choice of scale is always $\lesssim 10\%$.

Table 4
The predicted upper and lower limits on sparticle masses corresponding to left slepton mass 300 (400) GeV from curve 'e' ('f') of Fig. 5. The second and the third columns contain the input values of m_0 and $m_{1/2}$

Limit	m_0 (GeV)	$m_{1/2}$ (GeV)	$m_{\tilde{\chi}^\pm}$ (GeV)	$m_{\tilde{g}}$ (GeV)	$m_{\tilde{\chi}_1^0}$ (GeV)	$m_{\tilde{u}_L}$ (GeV)	$m_{\tilde{u}_R}$ (GeV)
Lower	265 (375)	200 (200)	135 (136)	506 (514)	76 (76)	497 (557)	487 (549)
Upper OL	195 (250)	334 (465)	245 (351)	793 (1074)	133 (189)	713 (963)	690 (931)
Upper CL	175 (224)	355 (494)	262 (374)	838 (1135)	142 (201)	746 (1009)	723 (974)

If gluinos happen to be the first sparticles to be discovered with a mass 700 GeV, say, it would predict that the lower bound on the slepton mass to be 265 GeV, as can be seen from line 'c' of Fig. 5.

The upper bounds in Table 4 indicate that the sparticle spectrum predicted by the mSUGRA model along with the requirement of the stability of the scalar potential can indeed be tested in future experiments. However, it is desirable that the theoretical predictions, the uncertainties due to the choice of renormalization scale in particular, be further sharpened. In this Letter we have followed Refs. [10,14] and assumed that the approximate scale, at which correct conclusions can be drawn from the tree level scalar potential, is equal to $M(\phi)^{\max}$ which is the dominant eigenvalue of the field dependent mass matrices. Our conservative limits on SUSY parameters are then obtained if these limits happen to be stable with respect to the variation of the scale within one order of magnitude of the above value.

In practice, however, the above eigenvalues may have a hierarchy. A more rigorous method [19] which takes into account this hierarchy and chooses the scale in a step by step fashion using the decoupling theorem [20] is called for. A refined estimation of the scale will be particularly important if the measured masses are found to be in conflict with the theoretical upper bounds after the discovery of SUSY.

Interesting predictions about some decay properties of sparticles also follow from Fig. 5. For example, below the curve marked 'b' the lighter chargino is the next lightest superparticle (NLSP). Thus a chargino of mass $\lesssim 160$ GeV is predicted to be the NLSP, since its contour marked 'd' in Fig. 5 lies below 'b' in the entire UFB3 allowed region. Consequently charginos with mass in this range can decay only via modes consisting of the LSP and SM particles. All decay channels involving on shell superparticles (e.g., $\tilde{\chi}^\pm \to e\tilde{\nu}$ or $\tilde{l}\nu$) are ruled out. In the mSUGRA scenario the mass of the

second lightest neutralino ($\tilde{\chi}_2^0$) closely follows that of the lighter chargino. Hence similar conclusion about the decay characteristic of $\tilde{\chi}_2^0$ can also be drawn.

At low $\tan\beta$, constraints derived from the UFB3 condition are not very sensitive to the sign of μ. In large $\tan\beta$ scenarios, $m_{1/2}^{\max}$ is more stringent for a given m_0. For $\mu < 0$, however, the constraint becomes moderately weaker compared to the $\mu > 0$ case. In the former case the SUSY radiative corrections to the bottom quark Yukawa coupling makes it smaller compared to its magnitude in the latter case. The effect of this coupling in the renormalization group evolution, which is quite significant in the large $\tan\beta$ scenario, is relatively subdued for $\mu < 0$. Thus the results presented in Figs. 3, 4 and in subsequent tables for $\mu < 0$ are conservative. We have checked that $m_{1/2}^{\max}$ may differ at most by 20 GeV due to the sign of μ.

In order to see whether the stability of the potential yields an improved absolute lower bound on the slepton masses compared to the experimental result, a more through scan of the parameter space is needed. This is beyond the scope of the present Letter. However, following comments can be made.

Since the main objective of this Letter is to combine the limits of [4] with the theoretical bounds obtained from the UFB3 condition, we restricted ourselves, as in [4] to $A_0 = 0$. For $A_0 < 0$, UFB3 bounds are more restrictive since $m_{H_u}^2$ becomes more negative [11]. Thus stronger results for $m_{1/2}^{\max}$ and $m_0^{\min}$ are expected. For $A_0 > 0$ results similar to the $A_0 = 0$ case are expected, at least for small $|A_0|$. Note that A_0 cannot have arbitrarily large positive values ($|A_0| < 3m_0$ from the CCB condition inequality (5) of [10]). In any case, a correlation between the limits on m_0, $m_{1/2}$ and positive A_0 is expected, which may have important predictions for the third generation of scalar superpartners.

Indirect constraints on the m_0–$m_{1/2}$ parameter space have been obtained [21,22] from the requirements that (i) the prediction of the mSUGRA model be

consistent with the dark matter density of the universe as given by the latest WMAP data [23], (ii) it removes the alleged discrepancy between the measured value of the $g - 2$ of the muon [24] and the standard model prediction or (iii) the prediction for the branching ratio of the inclusive process $b \to s\gamma$ be consistent with the measured value [25]. Cerdeno et al. [22] have also considered the impact of the UFB3 constraint on the parameter space. Our conclusions qualitatively agree with theirs.

For definiteness we compare the constraints obtained by Ellis et al. [21] based on the latest WMAP data [23] with our constraints. A precise comparison is difficult since the constraints in [21] are given for different sets of SUSY parameters. Yet the following qualitative remarks can be made.

From the relevant constrained parameter space for $\tan\beta = 10$, $A_0 = 0$ and both signs of μ can be found in Fig. (1a) and (1b) of [21]. Since our constraints are practically insensitive to the sign of μ for relatively small $\tan\beta$, the constrained parameter space of Fig. 2 of this Letter can be qualitatively compared with the results of [21]. It is interesting to note that for $\tan\beta = 10$ the dark matter and the m_h constraints allow only a very narrow region for low m_0 (~ 100 GeV) and relatively large $m_{1/2}$ ($\gtrsim 300$ GeV). This is very likely to be in conflict with the UFB3 constraint. Similarly for $\tan\beta = 35$, $\mu < 0$ and $A_0 = 0$, there is a tiny region allowed by both dark matter and $b \to s\gamma$ constraints corresponding to m_0 between 250–350 GeV and $m_{1/2} > 700$ GeV. For $\tan\beta = 35$ the UFB constraints are expected to be stronger than those presented in Fig. 3. Qualitatively one can estimate that the above regions will be disfavoured by the UFB3 constraints. We cannot comment on the compatibility of the large m_0 regions allowed by indirect constraints with the UFB3 condition without a fresh computation. The incompatibility between the post WMAP dark matter constraints and the UFB3 bound for relatively low $\tan\beta$ was also noted in [22] and we agree with them. On the basis of this observation $\tan\beta \lesssim 20$ was ruled out by the above authors. We note that such conclusions can be evaded by introducing a tiny R-parity violation which leaves the LSP essentially stable for collider experiments but unstable cosmologically. Such small effects can be naturally induced by higher dimension operators suppressed by a heavy mass scale. Thus values of $\tan\beta$ less than 20

are still very much relevant for the analysis of collider data.

Qualitatively one can also conclude that significant fractions of the UFB3 allowed parameter space, especially for relatively low m_0, will be disfavoured by the $b \to s\gamma$ constraint for all $\tan\beta$ and $\mu < 0$. For $\mu > 0$, on the other hand, the constraint from $b \to s\gamma$ is rather weak. In this scenario the region favoured by the $g - 2$ constraint has significant overlap with the UFB3 allowed parameter space for all $\tan\beta$.

Acknowledgements

References

[1] For reviews see, e.g., H.P. Nilles, Phys. Rep. 110 (1984) 1;
P. Nath, R. Arnowitt, A. Chamseddine, Applied $N = 1$ Supergravity, ICTP Series in Theoretical Physics, vol. I, World Scientific, Singapore, 1984;
H. Haber, G.L. Kane, Phys. Rep. 117 (1985) 75.
[2] A. Chamseddine, R. Arnowitt, P. Nath, Phys. Rev. Lett. 49 (1982) 970;
R. Barbieri, S. Ferrara, C. Savoy, Phys. Lett. B 119 (1982) 343;
L.J. Hall, J. Lykken, S. Wienberg, Phys. Rev. D 27 (1983) 2359;
N. Ohta, Prog. Theor. Phys. 70 (1983) 542.
[3] L.E. Ibanez, G.G. Ross, Phys. Lett. B 110 (1982) 215;
J. Ellis, D.V. Nanopoulos, K. Tamvaskis, Phys. Lett. B 121 (1983) 123;
L. Alvarez-Gaumé, J. Polchinski, M. Wise, Nucl. Phys. B 221 (1983) 495.
[4] ALEPH Collaboration, A. Heister, et al., Phys. Lett. B 544 (2002) 73.
[5] See, e.g., OPAL Collaboration, G. Abbiendi, et al., Phys. Lett. B 545 (2002) 272;
OPAL Collaboration, G. Abbiendi, et al., Phys. Lett. B 548 (2002) 258, Erratum;
OPAL Collaboration, I. Trigger, Int. J. Mod. Phys. A 16 (S1B) (2001) 807;
DELPHI Collaboration, T. Alderweireld, Int. J. Mod. Phys. A 16 (S1B) (2001) 775;
L3 Collaboration, P. Achard, et al., Phys. Lett. B 580 (2004) 37.
[6] CDF Collaboration, T. Affolder, et al., Phys. Rev. Lett. 88 (2002) 041801;

CDF Collaboration, T. Affolder, et al., Phys. Rev. Lett. 87 (2001) 251803;

D0 Collaboration, S. Abachi, et al., Phys. Rev. Lett. 75 (1995) 618;

For a review see, e.g., Report of the SUGRA Working Group for Run II of Tevatron, S. Abel, et al., hep-ph/0003154.

[7] For reviews of LEP results see, e.g., ALEPH, DELPHI, L3, OPAL Collaborations, N. De Filippis, Acta Phys. Pol. B 33 (2002) 3881;

LEPSUSYWG, ALEPH, DELPHI, L3, OPAL Collaborations, http://lep.susy.web.cern.ch/lepsusy/Welcome.html.

[8] R. Barbieri, G.F. Giudice, Nucl. Phys. B 306 (1988) 63.

[9] L. Alvarez-Gaumé, J. Polchinski, M. Wise, Nucl. Phys. B 221 (1983) 495;

J.M. Frere, D.R.T. Jones, S. Raby, Nucl. Phys. B 222 (1983) 11;

M. Claudson, L.J. Hall, I. Hinchliffe, Nucl. Phys. B 228 (1983) 501;

C. Kounnas, et al., Nucl. Phys. B 236 (1984) 438;

J.P. Derendinger, C.A. Savoy, Nucl. Phys. B 237 (1984) 307;

M. Drees, M. Glück, K. Grassie, Phys. Lett. B 157 (1985) 164;

J.F. Gunion, H.E. Haber, M. Sher, Nucl. Phys. B 306 (1988) 1;

H. Komatsu, Phys. Lett. B 215 (1988) 323.

[10] J.A. Casas, A. Lleyda, C. Munõz, Nucl. Phys. B 471 (1996) 3.

[11] A. Datta, A. Kundu, A. Samanta, Phys. Rev. D 63 (2001) 015008;

A. Datta, A. Samanta, J. Phys. G 29 (2003) 2721.

[12] A. Datta, A. Kundu, A. Samanta, Phys. Rev. D 64 (2001) 095016;

E. Gabrielli, K. Huitu, S. Roy, Phys. Rev. D 65 (2002) 075005;

D.V. Gioutsos, C.E. Vayonakis, JHEP 0301 (2003) 024.

[13] M. Claudson, L.J. Hall, I. Hinchliffe, Nucl. Phys. B 228 (1983) 501;

A. Kusenko, P. Langacker, Phys. Lett. B 391 (1997) 29.

[14] G. Gamberini, G. Ridolfi, F. Zwirner, Nucl. Phys. B 331 (1990) 331.

[15] ALEPH Collaboration, A. Heister, et al., Phys. Lett. B 526 (2002) 191.

[16] F. Paige, S. Protopopescu, H. Baer, X. Tata, hep-ph/0001086.

[17] See http://www.feynhiggs.de/, we have used the Feyn-Higgs1.2.1 program.

[18] See, e.g., W. de Boer, R. Ehret, D.I. Kazakov, Z. Phys. C 67 (1995) 647.

[19] D.V. Gioutsos, Eur. Phys. J. C 17 (2000) 675.

[20] K. Symanzik, Commun. Math. Phys. 34 (1973) 7;

T. Appelquist, J. Carazzone, Phys. Rev. D 11 (1975) 2856.

[21] J.R. Ellis, et al., Phys. Lett. B 565 (2003) 176;

U. Chattopadhyay, A. Corsetti, P. Nath, Phys. Rev. D 66 (2003) 035005, references to the earlier works can be found in these papers.

[22] D.G. Cerdeno, JHEP 0306 (2003) 030.

[23] C.L. Bennett, et al., astro-ph/0302207;

D.N. Spergel, et al., Astrophys. J. Suppl. 148 (2003) 175.

[24] Muon $g - 2$ Collaboration, G.W. Bennet, et al., Phys. Rev. Lett. 89 (2002) 101804.

[25] CLEO Collaboration, M.S. Alam, et al., Phys. Rev. Lett. 74 (1995) 2885;

Belle Collaboration, K. Abe, et al., hep-ex/0107065;

BaBar Collaboration, C. Lista, et al., hep-ex/0110010.